AJNR

Macroprolactinomas: serial MR imaging in long-term bromocriptine therapy.

P Lundin, K Bergström, R Nyman, P O Lundberg and C Muhr

AJNR Am J Neuroradiol 1992, 13 (5) 1279-1291
http://www.ajnr.org/content/13/5/1279

Macroprolactinomas: Serial MR Imaging in Long-Term Bromocriptine Therapy

Per Lundin,[1,3] Kjell Bergström,[1] Rickard Nyman,[1] Per Olov Lundberg,[2] and Carin Muhr[2]

PURPOSE: To study the changes in macroprolactinomas during long-term bromocriptine therapy by means of serial MR imaging, and to correlate the findings to the serum prolactin (S-PRL) levels. **PATIENTS AND METHODS:** Thirteen patients with macroprolactinomas were studied before and during bromocriptine therapy; six to 11 MR examinations were performed with a duration of follow-up of 22 to 74 months. Tumor size, extension, relationship to adjacent structures, and signal intensity patterns were evaluated. Signal intensity ratios and T2 values were calculated in areas of apparently solid tumor tissue. **RESULTS:** Bromocriptine effectively reduced the size of all tumors; the size reduction was already significant at 1 week, but often continued for several years. Reenlargement during therapy was seen in three cases. The development of chiasmal herniation parallel to increasing cisternal invagination into the sella was a common finding, but was not correlated to visual symptoms. Signal intensity patterns corresponding to hemorrhage, cysts or necrosis were frequently observed, and transitions from one pattern to another were common. Hemorrhage occurred mainly in tumors corresponding to high initial serum prolactin levels. After 1 year of therapy, there was a significant increase in T2 values, indicating an increased water content in residual solid tumor tissue. **CONCLUSIONS:** MR is valuable for follow-up in bromocriptine therapy of macroprolactinomas, and provides new information on the tumor size changes, the inner structure of the tumors, and the optic chiasm.

Index terms: Pituitary gland, neoplasms; Pituitary gland, magnetic resonance

AJNR 13:1279–1291, Sep/Oct 1992

Bromocriptine, an ergot derivative and dopamine receptor agonist, is widely accepted as the primary treatment for prolactin-secreting pituitary adenomas (prolactinomas) (1–4). In previous studies, with use of computed tomography (CT), the tumor has been found to decrease in size in the majority of patients on long-term therapy (1–5). Alterations in tumor attenuation that have been considered to represent the development of cysts or hemorrhages have also been reported (4–6). The reduction of the tumor size has been attributed to cell involution (7–10), but necrotic changes have also been claimed to occur (11–13).

Many reports have emphasized the value of magnetic resonance (MR) imaging as a tool in the assessment of pituitary macroadenomas (tumors with a minimum size of 10 mm), pointing out its ability to provide additional information over and above that yielded by CT (14–16). During bromocriptine therapy, variable MR characteristics have been observed in prolactinomas (17) that have been interpreted as involution of tumor cells, edematous tumor cells, and increased extracellular space (18). The MR findings have also been attributed to intratumoral hemorrhage (19, 20) and cysts (21). Signal intensity alterations have been noted on homogeneous tumor areas, in addition to the development of presumed cysts (21). However, as yet no systematic study using MR imaging has been reported for follow-up during long-term bromocriptine treatment of prolactinomas.

The purpose of this investigation was to study the changes in macroprolactinomas during long-

Received January 10, 1992; accepted contingent on revision February 27; revision received June 2.

This study was supported by grants from the Swedish Medical Research Council (project No. 6676).

Departments of [1] Diagnostic Radiology and [2] Neurology, Uppsala University, Akademiska sjukhuset, S-751 85 Uppsala, Sweden.

[3] Address reprint requests to Dr Per Lundin, Department of Diagnostic Radiology, Akademiska sjukhuset, S-751 85 Uppsala, Sweden.

AJNR 13:1279–1291, Sep/Oct 1992 0195-6108/92/1305-1279

TABLE 1: Patient data, S-PRL levels, duration of follow-up, tumor size and tumor reduction

Patient No.	Age (yr)/Sex	Initial S-PRL (μg/L)	Time of Normalization of S-PRL (mo)	Length of Follow-Up (mo)	Initial Tumor Size (cm^2)	Reduction of Tumor Size (%)	First Size Reduction at (wk)
1	51 M	142	3	74	3.8	76	6
2	64 F	2000	3	27	2.0	37	1
3	42 M	2800	18	65	7.0	51	6
4	48 F	3400	6	25	5.0	42	12
5	44 M	2200	18	58	11.2	85	1
6	39 M	3900	6	54	7.8	59	6
7	63 F	4800	12	51	10.8	46	27
8	63 M	1260	1.5	50	5.7	61	1
9	37 M	3600	n.n.	44	7.2	57	6
10	57 M	1150	n.n.	22	7.0	41	12
11	23 M	250	6	30	4.1	88	1
12	27 M	4200	6	32	14.1	88	4
13	59 M	3000	n.n.	22	5.5	65	1

Note.—The patients are numbered in the order of entry into the study. S-PRL, serum prolactin; n.n. = S-PRL reduced, but not normalized.

term treatment with bromocriptine by means of serial MR imaging, and to correlate the findings to the serum prolactin (S-PRL) levels.

Patients and Methods

Thirteen patients, 10 men and three women, with prolactin-secreting macroadenomas, who had not previously been treated with dopamine agonists, were evaluated prospectively. They constituted a consecutive series referred to the Department of Neurology during a 4.5-year period. Their mean age was 47.5 years (Table 1). The findings in five of the patients have been partially included in a preliminary report (21).

The diagnosis was established clinically and radiologically. In four patients, it was verified histopathologically; three of the specimens were obtained surgically and one by transsphenoidal fine-needle aspiration (22). The initial maximal S-PRL level varied between 142 and 4800 μg/L (normal ≤20 μg/L) (Table 1). Growth hormone levels were normal in all cases. Eleven patients had not received treatment previously. Two patients had undergone surgery, and one of them had received radiotherapy postoperatively; both of these patients had large residual tumors.

Bromocriptine therapy was initiated by intramuscular injection of either of two slow-release preparations (Parlodel LA (long-acting) and Parlodel LAR (long-acting repeatable), Sandoz, Basel, Switzerland), with subsequent oral treatment; informed consent was obtained in all cases. Clinical examinations were performed repeatedly, with measurements of S-PRL and examination of the visual fields. MR examinations were performed 0–20 days before treatment (n = 12, not done in patient 12), and approximately 1 week (n = 11) and 1.5 (n = 13), 3 (n = 10), and 6 (n = 13) months after the first dose of bromocriptine. Thereafter, an approximately 1-year follow-up study was carried out at 10–15 months (n = 13), a 2-year study at 18–30 months (n = 12), and a 4- to 6-year study at 44–74 months (n = 7). The duration of follow-up varied between 22 and 74 months (Table 1) and the number of MR studies between 6 and 11 (total 108). CT examinations were carried out before the start of therapy in all patients.

MR imaging was performed by using a superconductive unit (Magnetom, Siemens AG, Erlangen, Germany), operating at 0.35 T in the first four examinations in two patients, and otherwise at 0.5 T. Using a head-coil, multisection spin-echo images were obtained with a section thickness of 10 mm with a 0- to 10-mm intersection gap in 36 examinations, and of 5 mm with a 0- to 1-mm gap in 72. In all examinations, sagittal T1-weighted images were obtained using 500/30-35/2 (TR/TE/excitations) (300/35/4 at 0.35 T), and frontal proton density- and T2-weighted dual-echo images, 1500-1800/30-35,90-120/1-2. In seven patients, the same parameters of the dual-echo sequence were used in all examinations, and in six patients the parameters of the T2-weighted images were 1500/120 in the first 1–4 examinations and 1500/90 in the others. Sagittal 1500/30-35,90-120/1 images were obtained in seven patients (35 examinations), and axial 500/30/2 or 1500/30-35,90-120/1 images in all patients (94 examinations). The acquisition matrix was 256 × 256 and the field of view was 30 cm. In addition, nine patients were examined with a sagittal multiecho single-section sequence 1500/30-240/1, eight evenly spaced echoes, and an acquisition matrix of 128 × 256 or 256 × 256 (57 examinations). Eleven examinations in six patients (all of them included the last examination) were also performed after intravenous administration of Gd-DTPA (0.1 mmol/kg), with both frontal and sagittal T1-weighted images in five examinations, and only sagittal images in six.

All images were evaluated by two neuroradiologists (P.L. and K.B.) by consensus. Tumor size changes were estimated both visually and quantitatively. In the quantitative estimation, a central sagittal T1- (n = 11) or frontal proton

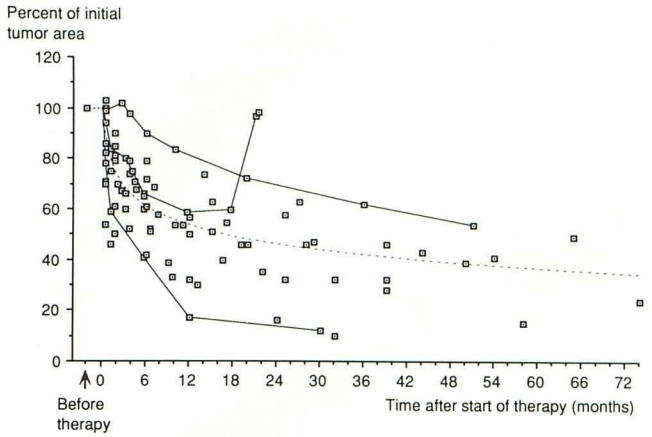

Fig. 1. Scatter diagram of the percentage of the initial tumor area plotted against time (all patients). A logarithmic curve is fitted (*dashed line*). Tumors showing slow regression (patient 7), tumor reexpansion (patient 10) and rapid regression (patient 11) are indicated by lines from top to bottom, in that order.

density-weighted (n = 2) image was chosen, and displayed at 2× magnification. The tumor area was measured by outlining the tumor with a pen-guided cursor. The window settings were chosen subjectively to optimize image contrast. Similar patient positions and section levels were used in the follow-up studies, and a tumor size ratio was calculated as the ratio between the tumor area in a follow-up study and that in the initial study. In patient 12, the initial tumor area was measured on a frontal CT image.

The evaluation included the tumor extension and the relationship to the cavernous sinus and the base of the skull; cavernous sinus invasion was considered to be present when the internal carotid artery was encased by the tumor (23). The relationship of the tumor to the optic chiasm was evaluated. Downward angulation into the sella of the optic chiasm and optic nerves was considered to represent chiasmal herniation (24). The signal intensity patterns of the tumors were classified into three types. Signal intensity similar to that of cerebral gray matter in all sequences was regarded as the "solid" type of intensity pattern. Increased signal intensity relative to gray matter in all sequences was designated as the "hemorrhagic" type (25, 26). The third type of pattern was characterized by high signal intensity in the T2-weighted image with low or intermediate intensity in corresponding areas of the T1-weighted image, and was considered to represent an increased water content (27); this is referred to in the following as an "increased water" type of pattern. Tumors with the solid type of intensity pattern only were regarded as homogeneous, and other tumors as inhomogeneous.

MR parameters were measured on areas with the solid type of intensity pattern. Measurements were made on midsagittal T1-weighted images and on frontal (n = 11) or sagittal (n = 2) proton density- and T2-weighted images. Circular regions of interest (ROIs) comprising 13–57 pixels were placed in the tumor and also in the anterior part of the pons and in the splenium of the corpus callosum (sagittal images), and in the body of the corpus callosum (frontal images). Signal intensity ratios of tumor to corpus callosum, and in the T1-weighted image also of pons to corpus callosum, were calculated at examinations performed at 0.5 T. From the multiecho sequence, a T2 image was calculated using the software option of the equipment (Numaris, Siemens AG), assuming monoexponential processes. T2 values were also calculated from the dual-echo images using an algorithm given by Sperber et al (28). The signal intensity ratio of pons to corpus callosum in the T1-weighted image and the T2 values of the corpus callosum (sagittal and frontal sequences) and pons (sagittal sequences) were used as references.

The results were analyzed statistically with the Wilcoxon sign-rank test, one-way analysis of variance, Fisher's exact test, and linear regression. Probabilities below .05 were accepted as indicating significance.

Results

Tumor Size and S-PRL Levels

The visual and quantitative estimations of the changes in tumor size were in close agreement in all patients. The third axis of the tumor that was not included in the quantitative assessment visually paralleled the changes in the central tumor area, or remained unchanged. All tumors diminished in size, the maximum reduction ranging between 37% and 88% (mean 61.2%) (Table 1). A scatter diagram with the tumor size ratio plotted against time for all patients is given in Figure 1. In patient 12, both MR and CT were performed at the first follow-up, and the tumor size measured at the two examinations differed by less than 5%.

Visually, a size reduction was evident at 1 week in five patients, and at 1–6 months in the other eight. There was an approximately 50% reduction at 1–6 weeks in three patients (Fig. 2). Statistically, the tumor size was significantly diminished already at 1 week ($P = .015$, Wilcoxon sign-rank test), and later the significance was stronger.

In two patients, steady state was achieved without any further detectable changes in tumor size after 12–17 months; in eight patients, the size reduction continued throughout the period of follow-up (Fig. 2); and in three patients, there was an increase in tumor size after an initial decrease. In one of these, an area of the "hemorrhagic" type of intensity pattern had increased in size at the last examination, with slight expansion of the tumor (Fig. 3). In another patient (patient 10), the tumor size had decreased by 41% 1 year after the start of therapy, but at 2 years it had almost regained the initial size (Fig. 1) and there was a

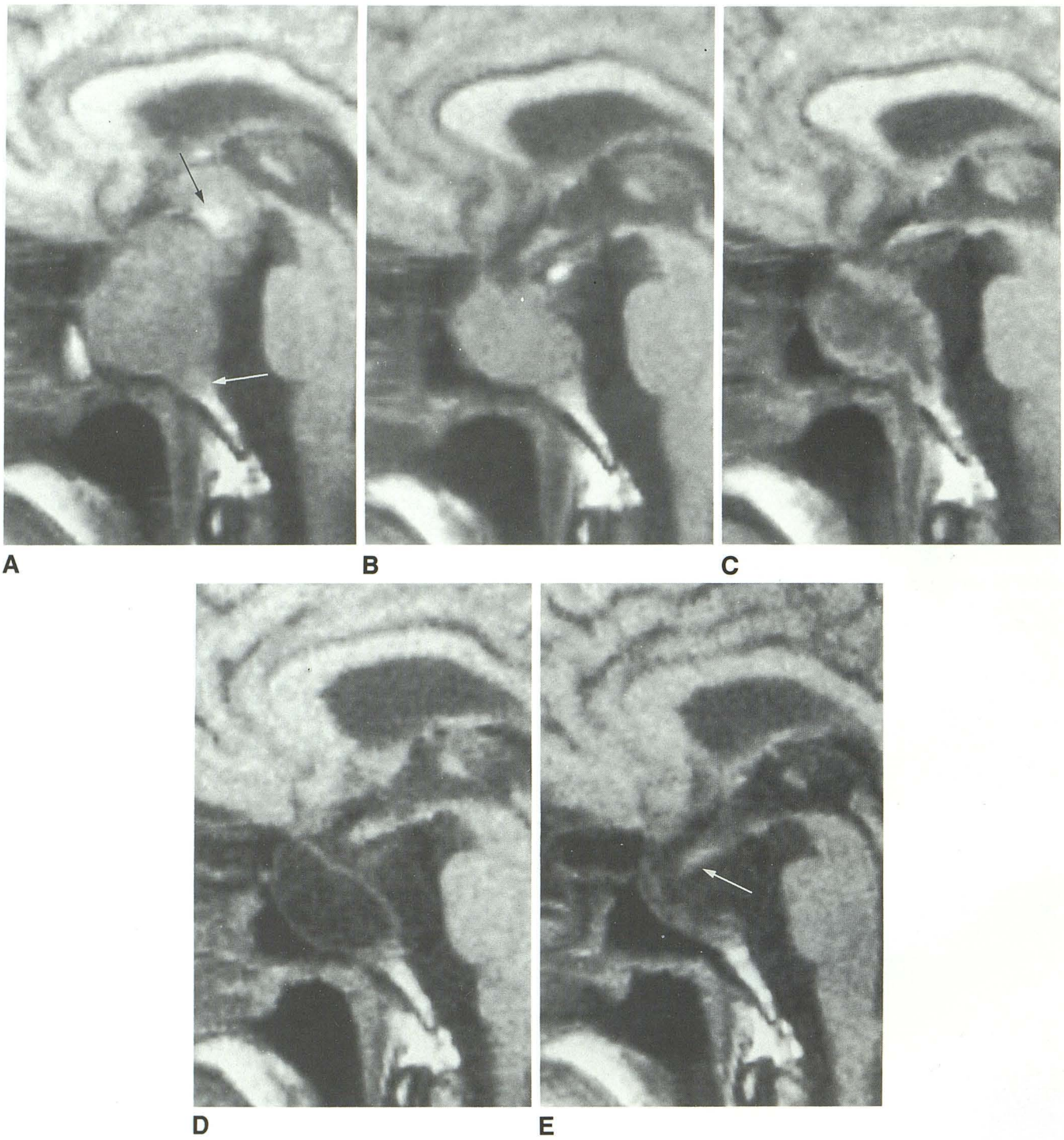

Fig. 2. Patient 5. T1-weighted (500/30) sagittal images.

A, Before therapy. There is a large suprasellar portion of the tumor, containing an area of presumed hemorrhage (*black arrow*). The tumor extends into the clivus (*white arrow*).

B, At 1 week. Most of the suprasellar portion has disappeared. The chiasm reaches to the level of the sellar entrance plane.

C, At 3 months. A central hypointense, irregular area has developed (moderately hyperintense in a T2-weighted image, not shown). The area of hemorrhage has disappeared.

D, At 28 months. In the center of the tumor there is a hypointense area with a thin surrounding rim. Because of increasing headaches, a transsphenoidal fine-needle aspiration was performed, and yielded 4 mL of colorless fluid.

E, At 58 months. There is a thin, slightly irregular area of residual tissue in the sella. The chiasm (*arrow*) is herniated into the sella, and the optic recess of the third ventricle is elongated.

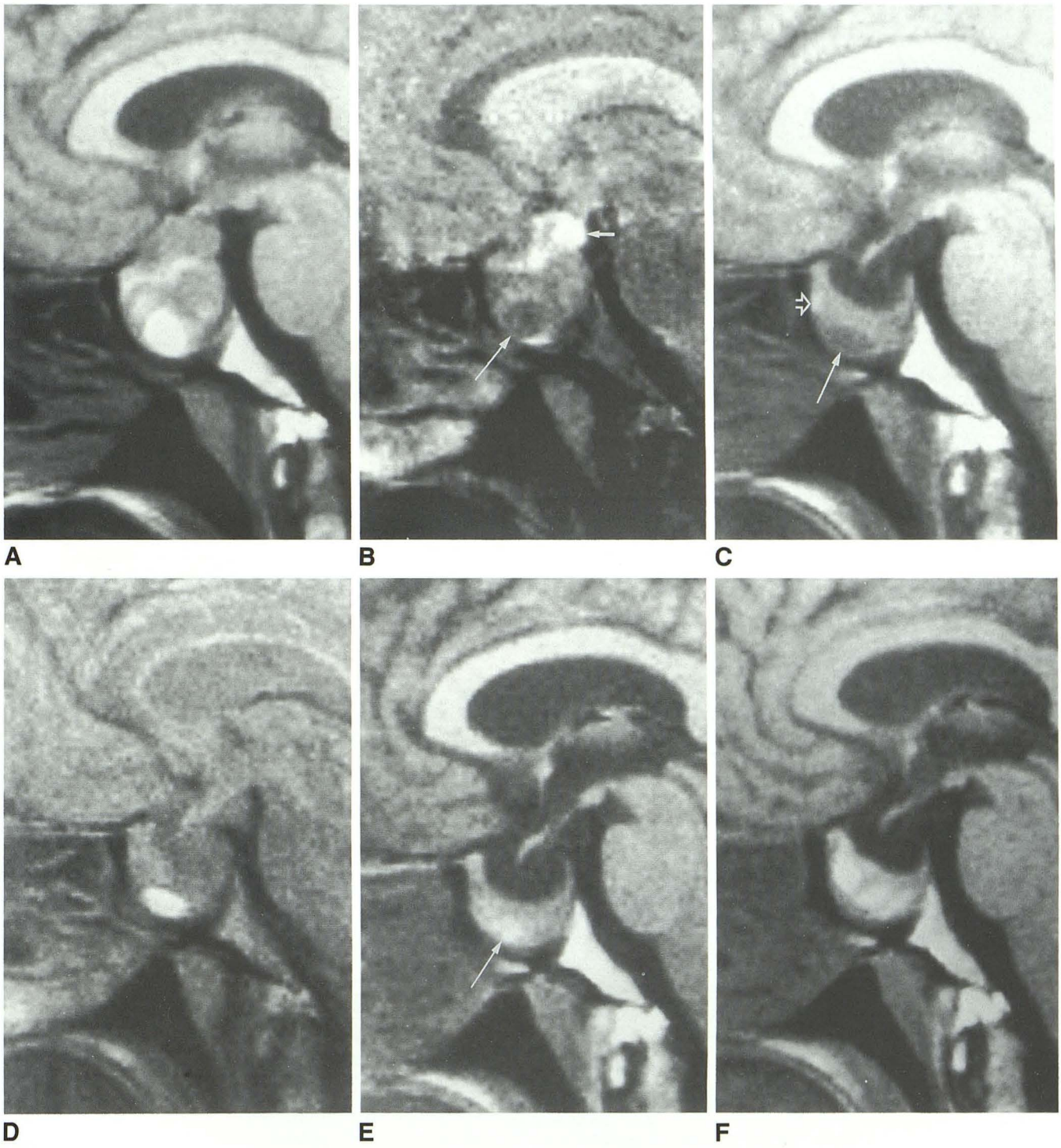

Fig. 3. Patient 3.

A and *B*, T1- (500/30) and T2-weighted (1500/120) sagittal images before therapy. There are areas of presumed hemorrhage within the tumor; the lower area with high signal intensity in the T1-weighted image corresponds to mixed, mainly slightly low intensity in the T2-weighted image (*long arrow*). There is also an area of the "increased water" type (*short arrow*).

C and *D*, T1- and T2-weighted (1500/90) sagittal images at 1 year. The tumor has decreased considerably in size. The intrasellar area of presumed hemorrhage now has the appearance of a cyst (*long arrow*). There is slight residual hyperintensity in the T1-weighted image (*open arrow*).

E, A T1-weighted sagittal image at 30 months shows further size reduction. Again, a small area of presumed hemorrhage is seen inferiorly (*arrow*). The chiasm reaches to the level of the sellar entrance plane.

F, T1-weighted sagittal image at 65 months. The tumor size has increased slightly and there are now larger areas of presumed hemorrhage.

fourfold increase of the S-PRL level compared with the lowest value. Because of increasing visual impairment the patient then underwent surgery, and solid tumor tissue was found (he was thereafter excluded from the study). In the third patient (patient 12), there was a 54% size reduction at 1 month, but at 3 months the tumor had reexpanded and at 7 months reached 75% of the initial size, while S-PRL was lowered to a normal level. Visual deterioration occurred, corticosteroid therapy was initiated, and a transsphenoidal fine-needle aspiration was performed, which yielded 2 mL of blood-stained fluid. Thereafter, during continued bromocriptine treatment, the tumor size gradually diminished, reaching 12% of the initial size.

The S-PRL levels decreased rapidly in all patients, and after 3–18 months it had reached a normal level in 10 of them. The reduction of S-PRL always preceded the reduction of the tumor size.

Tumor Extension and Adjacent Structures

Initially, 10 tumors showed suprasellar extension, and the optic chiasm was displaced in all these cases. The suprasellar portion of the tumor disappeared completely during treatment in nine cases, and in eight of these the optic chiasm had herniated into the sella (n = 3) or the sellar entrance plane (n = 5) at the end of follow-up (Figs. 2, 3, and 4). In one patient without suprasellar extension, herniation of the chiasm was found before therapy, and, in this case, the herniation into the sella increased with reduction of the tumor size (Fig. 5). In the T2-weighted image, high signal intensity was observed in the chiasm at the end of follow-up in this patient and in two further patients with marked herniation (Fig. 4). In all cases of chiasmal herniation, the suprasellar cistern became invaginated into the upper part of the sella (partially empty sella). The herniation paralleled the increasing sellar invagination of the suprasellar cistern. Invagination of the suprasellar cistern was also seen in three patients in whom the optic chiasm appeared normal. There was no visual deterioration in any of the patients with chiasmal herniation; two of them had no visual disturbances at all, and six had visual field defects initially that disappeared or improved during treatment.

Signs of tumor invasion of the cavernous sinus and/or the base of the skull were found in nine patients. As estimated visually, the size of the tumor portion in the cavernous sinus paralleled the changes in size of the total tumor. Tumors located in the base of the skull diminished concentrically or eccentrically (Fig. 5), with increasing aeration of the sphenoid sinus.

Signal Intensity Patterns

Before therapy, five tumors were homogeneous and eight were inhomogeneous, corresponding to 10 areas of inhomogeneity (two tumors having both the "hemorrhagic" and "increased water" types) (Fig. 6). Eight new focal areas of inhomogeneity appeared in seven patients; four of these areas were of the increased water type (one verified as a cyst by transsphenoidal fine-needle aspiration, Fig. 2), and four were of the hemorrhagic type. Twelve areas disappeared during bromocriptine therapy—five of the increased water type and seven of the hemorrhagic type. Changes between the hemorrhagic and the increased water types of intensity pattern were common (Figs. 3 and 7). On a total of nine occasions in seven patients, new areas of the hemorrhagic type or changes into this type were noted. Two initially homogeneous tumors remained so throughout the follow-up period.

Most areas of inhomogeneity appeared during the first 6 months of therapy (Fig. 6), but two new areas were noted after 1 year or more. One area of the hemorrhagic type persisted for 1 year, five were present for 3–6 months, and seven were seen at one examination only. In one patient (patient 7), a lesion of the hemorrhagic type preceded any demonstrable change in tumor size, but, otherwise, changes of the signal intensity patterns occurred at the same time or later than the first reduction in tumor size.

Hyperintensity in the T1-weighted image with corresponding hypointensity in the T2-weighted one was seen initially in one patient (Fig. 3); later, there was hyperintensity in both images. Disappearing areas of the hemorrhagic type turned into hypointense areas on T2-weighted images in three cases, in one of them with a ringlike shape.

Most areas of the hemorrhagic type were small. Larger areas occurred among those of the increased water type and among those changing between the two types. In addition to the previously mentioned tumor reenlargement in patient 3, temporary expansion of part of the tumor adjacent to an area of the hemorrhagic type occurred in patient 7 (Fig. 7); both lesions were clinically silent. There was no tumor reexpansion associated with the increased water type of intensity pattern. In one patient, an opening was seen

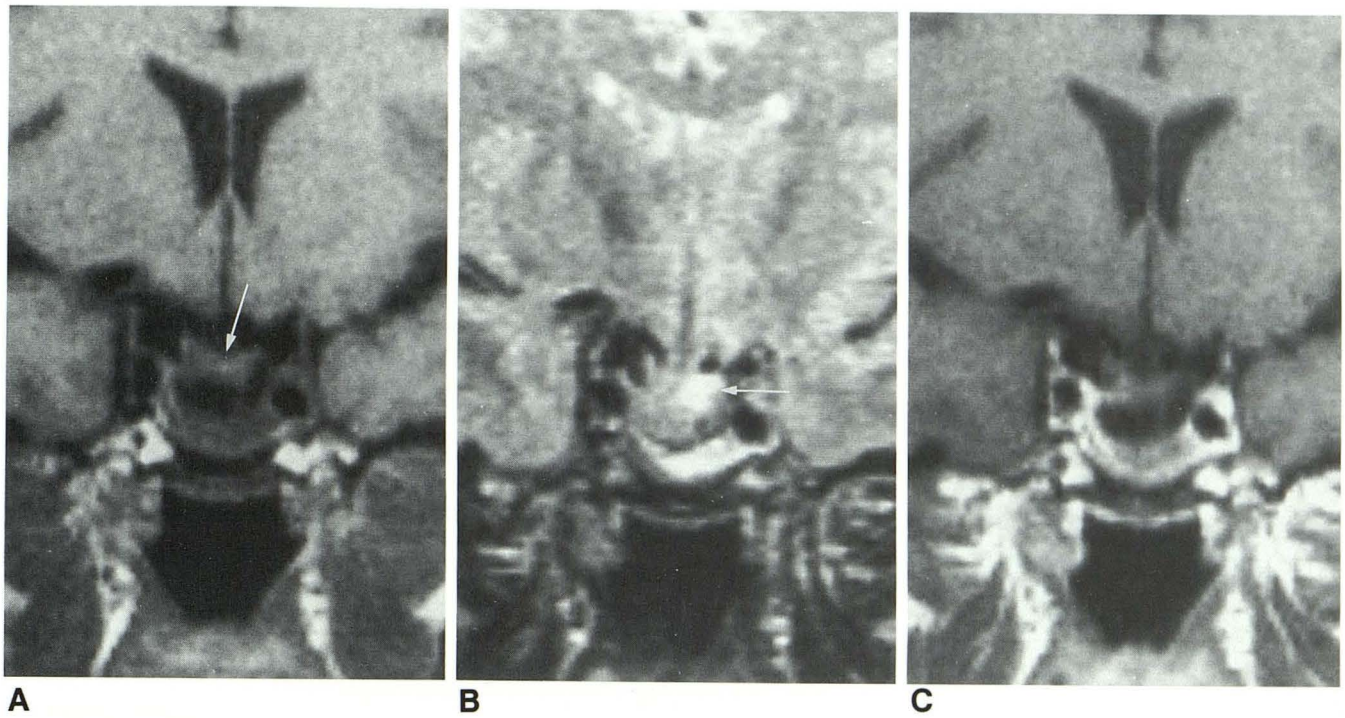

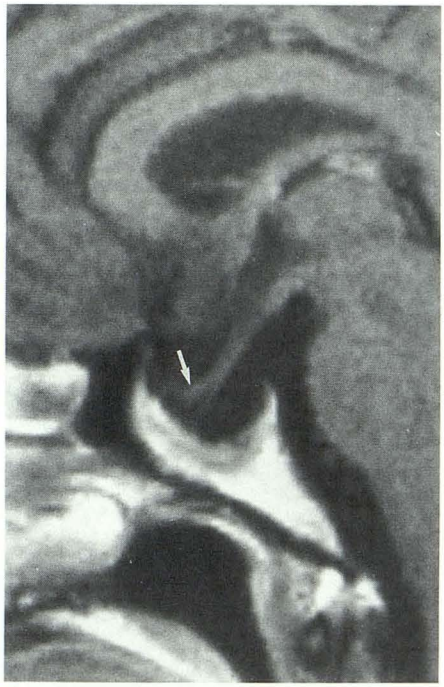

Fig. 4. Patient 12. All images are from the 2-year follow-up. Initially, the tumor had a large suprasellar portion.

A, Frontal T1-weighted (500/30) image. There is residual tumor in the lower part of the sella and invagination of the suprasellar cistern in the upper part. The chiasm (*arrow*) is herniated into the sella.

B, Corresponding T2-weighted image (1800/90). The bulk of the tumor is hyperintense. There is also hyperintensity in the left-hand part of the chiasm (*arrow*).

C, Frontal Gd-DTPA-enhanced T1-weighted image. The tumor is enhancing, though irregularly, with less pronounced enhancement centrally.

D, Sagittal contrast-enhanced T1-weighted image. There is marked herniation of the optic chiasm (*arrow*) and elongation of the third ventricle.

to develop between an area of the increased water type and the suprasellar cistern, resulting in intrasellar invagination of the cistern.

Measurements of MR Parameters

Nine examinations were excluded from the analysis of MR parameters, two for technical reasons (damaged magnetic tape), and seven because there were only minor visible areas of the solid type of intensity pattern (three patients). In addition, from the eight examinations performed at 0.35 T, the signal intensity ratios were not calculated, but calculations were made of T2 values from dual-echo sequences. Visually, diffuse moderate hyperintensity in the T2-weighted image developed in six tumors (Fig. 5), and it was doubtful whether these areas should be char-

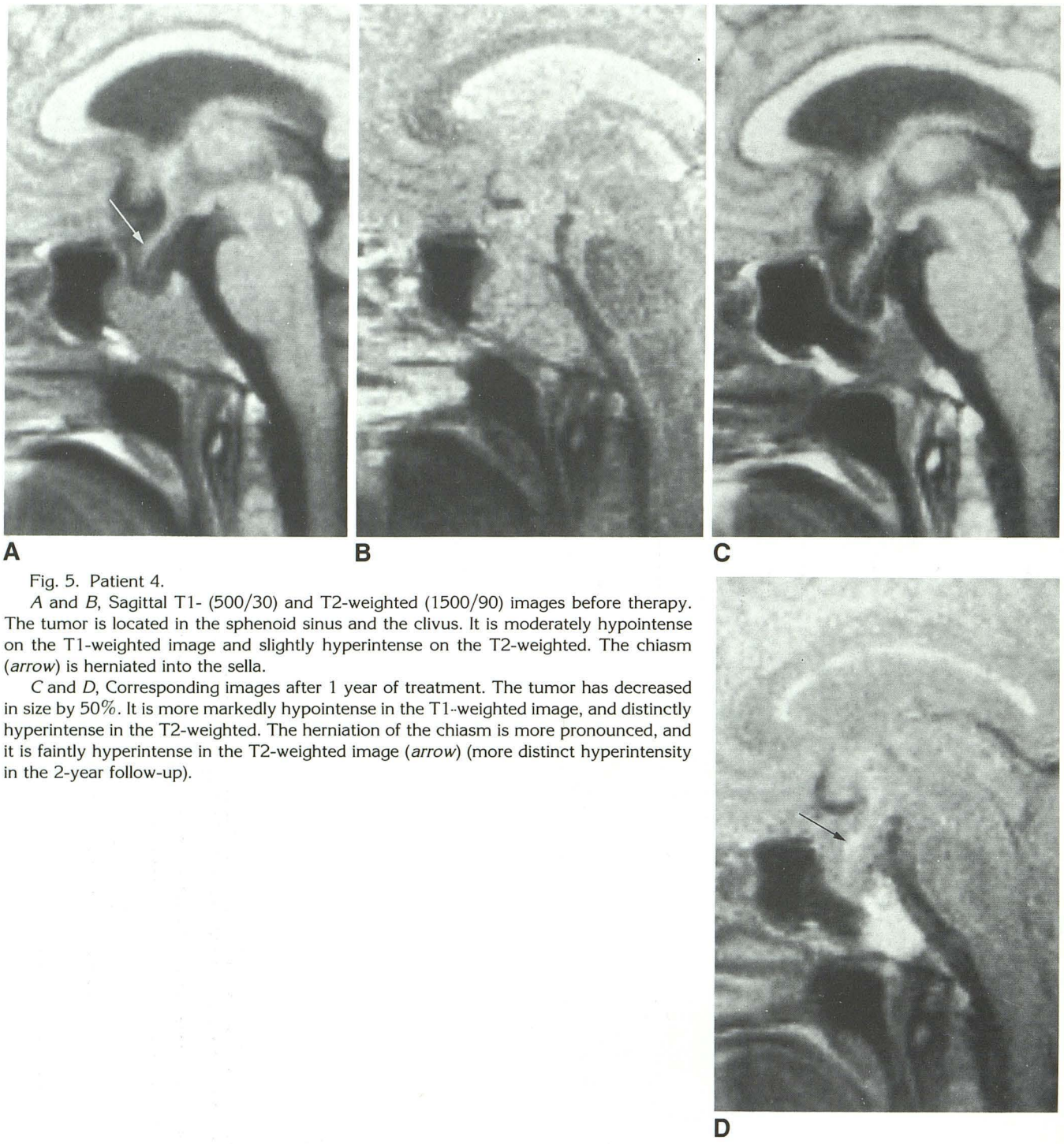

Fig. 5. Patient 4.

A and *B*, Sagittal T1- (500/30) and T2-weighted (1500/90) images before therapy. The tumor is located in the sphenoid sinus and the clivus. It is moderately hypointense on the T1-weighted image and slightly hyperintense on the T2-weighted. The chiasm (*arrow*) is herniated into the sella.

C and *D*, Corresponding images after 1 year of treatment. The tumor has decreased in size by 50%. It is more markedly hypointense in the T1-weighted image, and distinctly hyperintense in the T2-weighted. The herniation of the chiasm is more pronounced, and it is faintly hyperintense in the T2-weighted image (*arrow*) (more distinct hyperintensity in the 2-year follow-up).

acterized as the solid type of intensity pattern or the increased water type, but they were included in the analysis of MR parameters. Four of these patients were examined after administration of Gd-DTPA, and the hyperintense tumor areas all showed enhancement (Fig. 4).

The coefficient of variation of the pixel values within the ROIs did not exceed 20%; in most cases, it was less than 10%. The calculated T2 values of the corpus callosum did not differ significantly between the 1500/35,120 (0.35 T), 1500/30-35,90 (0.5 T), 1500/35,120 (0.5 T) and 1800/30,90 (0.5 T) sequences (one-way analysis of variance; mean values (SD) 77.9 (7.6), 73.6 (5.9), 71.6 (8.0), and 71.7 (7.3) msec, respectively), and the T2 values obtained from the four

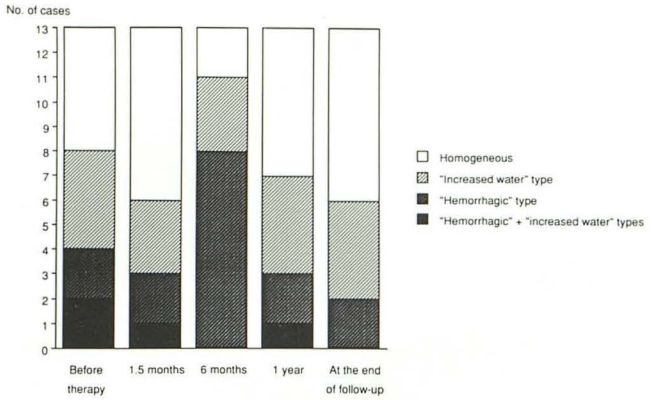

Fig. 6. The number of homogeneous and inhomogeneous tumors before and during bromocriptine therapy, and at the end of follow-up. In patient 12, the classification regarding the baseline examination was based on CT, which showed a hypodense, nonenhancing area that was considered to be an area of the "increased water" type.

sequences, therefore, were analyzed together. For each patient, the coefficient of variation of the references during the period of follow-up was calculated. It was found not to exceed 10% either for the pons/corpus callosum signal intensity ratio (T1-weighted image), or for the T2 values of the corpus callosum (dual- or multiecho sequences) and pons (multiecho sequence). The reference values did not differ significantly between the baseline and any of the follow-up examinations (Wilcoxon sign-rank test) (Fig. 8).

The results of the analysis of the MR parameters are summarized in Table 2 and Fig. 8. The mean tumor/corpus callosum signal intensity ratio in the T1-weighted image increased slightly in the first 6 months but had decreased again at 1 and 2 years; the changes were not significant. The signal intensity ratio was increased by 20%–40% at 3–6 months in two patients (patients 8 and 12; in the latter case in comparison with the 1-month follow-up). The signal intensity ratio in the proton density-weighted images did not change significantly; in the T2-weighted image there was an increase in seven patients (statistical analysis was not performed due to the variable sequences) (Table 2). T2 values based on both the dual-echo (Fig. 8) and the multiecho sequences were increased at the 1- and 2-year examinations. The multiecho sequence value at 1 year differed significantly from the pretreatment value, and the same applied to the dual-echo sequence at 2 years ($P = .028$ and .015, respectively, Wilcoxon sign-rank test). T2 did not increase in all patients; in patients 2 and 3 it changed only slightly. In patient 10, it was reduced by 20% at 6 months, with a subsequent slight increase. Patient 11 showed a 30% decrease in T2 (dual-echo) at 1.5 months; thereafter, it could not be measured. In five patients, the T2 value at 4–6 years was similar to the 1- and 2-year values, and, in one patient, it was lower.

Correlation between the Parameters

The average size reduction in the group of three tumors without suprasellar extension was smaller than in the group of 10 tumors with initial suprasellar extension; the three former patients were all women and the latter were all men. Areas with the hemorrhagic type of intensity pattern developed more often in tumors associated with an initial S-PRL level exceeding 2500 μg/L than in those associated with lower S-PRL levels (six/seven vs one/six, $P < .05$, Fisher's exact test). No further correlation was found between the initial tumor parameters, ie, S-PRL, tumor size, tumor extension, signal intensity patterns, and MR parameters, and the tumor parameters during bromocriptine therapy, ie, time taken for normalization of S-PRL, maximal tumor size reduction, rate of size reduction, appearance of areas of inhomogeneity, and MR parameters. The latter parameters did not correlate to each other.

Discussion

In this series, bromocriptine treatment of macroprolactinomas was found to be effective, in accordance with previous reports (1–4). Using serial MR imaging, new and clinically important information was obtained, both regarding the tumor size changes, the optic chiasm, and changes within the tumors. In addition, the time of follow-up was longer than in prior studies (1–5), which also provided a new perspective on the effects of bromocriptine on prolactinomas.

We found a high frequency (six out of seven cases) of further tumor shrinkage after 2 years of follow-up, indicating that prolonged treatment is meaningful. A similar finding has not been reported previously to our knowledge, which might be related to the longer time of follow-up in our series than in previous studies relying on CT (1, 3, 5), and possibly also to a higher sensitivity of MR than CT in detecting small changes in tumor size. Otherwise, the tumor size changes correspond roughly to those observed in previous studies (1, 3, 5), but a more than 80% reduction has only rarely been reported (29). Rapid tumor

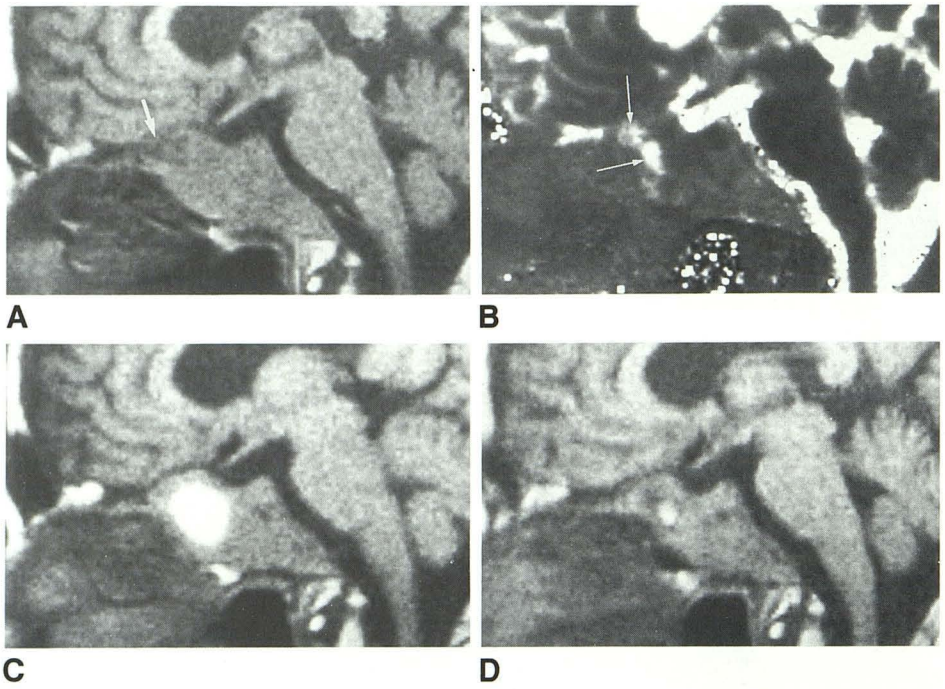

Fig. 7. Patient 7.

A, Sagittal T1-weighted (500/35) image before therapy. The tumor is located in the base of the skull. There is a slightly hypointense area anteriorly (*arrow*).

B, Corresponding calculated T2-image from the multiecho sequence 1500/30-240. High T2 values are found in the anterior part of the tumor (*arrows*), and extend more caudally than the hypointense area in *A*. The ROI was placed in the posterior part of the tumor.

C, Sagittal T1-weighted (500/35) image at 6 months. An area of presumed hemorrhage has appeared in the anterior part of the tumor. The superior part of the tumor adjacent to the hemorrhagic area is bulging locally; but the tumor area has decreased by 10%.

D, Sagittal T1-weigthed (500/35) image at 10 months. The area of presumed hemorrhage has decreased, and a hypointense peripheral zone is now seen (hypointensity in T2-weighted images also, not shown). The anterior part of the tumor is smaller. There are irregular, slightly hypointense areas posteriorly.

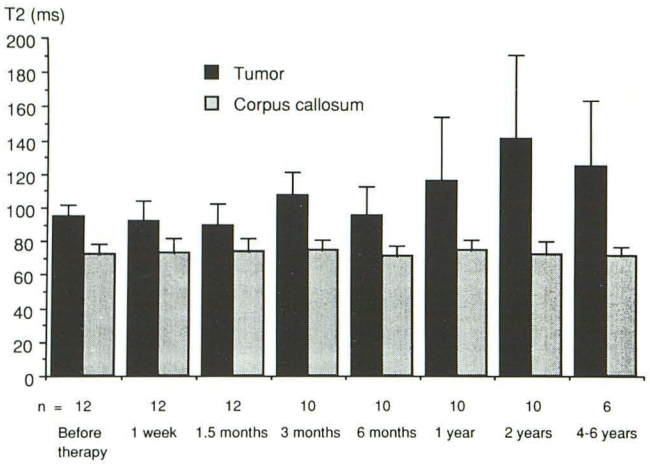

Fig. 8. Mean T2 (SD) of the tumor and of the corpus callosum, calculated from the dual-echo sequence. n = number of patients forming the basis of the graph.

regression has previously been described (29, 30), and was not infrequent in parenteral bromocriptine therapy. Neither the basal S-PRL level nor the initial tumor size could predict the final degree or the rate of tumor size reduction. Tumors with suprasellar extension were associated with a more marked size reduction than those that mainly grow in the base of the skull, but the number of patients was small and there was also a difference in sex distribution between the two groups.

The tumor size changes were estimated by a two-dimensional model, which has been shown to correlate strongly to the tumor volume (31). The comparison between the patients regarding the initial tumor size must be regarded as a rough approximation (31).

To our knowledge, chiasmal herniation into the sella as a result of bromocriptine therapy has not previously been reported. A possible cause of this herniation might be adhesions between the suprasellar portion of the tumor and the chiasm, resulting in traction of the chiasm with reduction of the tumor size. The development of high signal intensity in the chiasm in the T2-weighted image indicates an increased water content. Whether this reflects edema, gliosis, or other histologic changes is uncertain. None of our patients had visual disturbances that could be attributed to the chiasmal herniation, but visual symptoms have been found to be associated with chiasmal herniation in primary empty sellae (24). In the event of visual deterioration during bromocriptine treatment of macroprolactinomas, chiasmal herniation, therefore, must be considered as an alternative cause in addition to tumor reexpansion.

TABLE 2: Signal intensity ratios and T2 before and after 2 years of therapy

Patient No.	Signal Intensity Ratio (tumor/corpus callosum)				T2 (msec)			
	TR/TE (500/30–35)		TR/TE (1500–1800/90–120)		From Dual Echo		From Multiecho	
	Before Therapy	After 2 (4–6) yr	Before Therapy	After 2 (4–6) yr	Before Therapy	After 2 (4–6) yr	Before Therapy	After 2 (4–6) yr
1	–	(0.84)	–	1.28	93	134	–	–
2	–	0.84	–	1.17	98	110	–	–
3	0.89	0.87	1.38	1.29	92	83	112	130
4	0.85	0.60	1.31	1.66	96	230	130	–
5	0.84	0.87	1.30	1.50	94	200	141	243
6	0.77	–	1.18	–	99	–	173	–
7	0.74	0.85	1.12	1.58	107	125	145	(207)
8	0.76	(0.69)	1.12	(1.63)	93	(175)	159	–
9	0.74	0.77	1.26	1.50	98	111	113	253
10	0.81	0.87	1.05	1.41	101	103	120	141
11	0.73	–	1.56	–	93	–	169	–
12	–	0.75	–	1.59	–	196	–	–
13	1.07	1.01	1.40	1.43	78	119	–	–

Note.—Dashes represent examinations that were not performed or that were impossible to analyze quantitatively. Values in parentheses = no value available at 2 years; the value from the 4- to 6-year follow-up is entered.

This differential diagnosis will readily be resolved by MR.

Areas of hyperintensity in all sequences probably corresponded to subacute or chronic hemorrhage (25, 26), and the hyper- and hypointense area in the T1- and T2-weighted images, respectively, seen in patient 3 most likely represented more recent hemorrhage (32). Areas of low and high signal intensity in the T1- and T2-weighted images, respectively, were seen in seven patients, ie, an appearance typical of tumoral cysts (33). In three patients, there was isointensity in the T1- and hyperintensity in the T2-weighted images. The histologic basis of these areas is more obscure. The increased signal intensity in the T2-weighted image indicates a high water content (27), supporting the possibility of necrosis or cysts, and a relatively large number of such areas have previously been found to correspond to nonenhancing areas on CT (15).

Areas of presumed hemorrhage, cysts, or necrosis developed frequently. Using CT, Wolpert (5) found a similar frequency of development of low-density areas in macroprolactinomas during bromocriptine therapy. MR revealed a dynamic course with transitions from one type of degenerative change to another. Yousem et al (19) reported that 50% of their patients with prolactinomas undergoing treatment with bromocriptine showed intratumoral hemorrhage. Similarly, we found a high incidence of hemorrhage, but in our study, new information on the changes over time was obtained, and a particularly high prevalence of hemorrhagic tumors was noted after 6 months of therapy. The pituitary apoplexy syndrome has been observed in patients with prolactinomas during treatment with bromocriptine (34, 35). We observed slight tumor reexpansion, local or generalized, due to intratumoral hemorrhage in two patients, but neither of them had any clinical symptoms. Scotti et al (4) also found tumor reexpansion that was probably due to hemorrhage in two out of 28 patients. All of these findings indicate that, in patients with macroprolactinomas receiving bromocriptine, there is a risk of tumor expansion due to hemorrhage, even after 5 years of therapy. Close clinical surveillance, therefore, is indicated.

The relative stability of the MR reference parameters indicate that the reproducibility of the measurements is reasonably good, in accordance with the findings in previous studies in which relaxation times were calculated from similar sequences (36, 37). However, the signal intensity ratio in the T2-weighted image was derived from various sequences and a reference was lacking, which rendered the analysis of this parameter difficult.

The histologic basis of the regression of prolactinomas during bromocriptine therapy has not yet been definitely settled. The size reduction has been attributed by some authors to cell involution

(7–10), and other studies have indicated that necrosis also occurs (11–13). Bassetti et al (8) found a 39%–47% reduction in cell area in adenomas from patients treated for up to 1 year. The connective tissue stroma of prolactinomas has been reported by several authors to increase during bromocriptine therapy (8, 12, 39). In view of these results, our finding of a 80%–90% tumor area reduction is difficult to explain, except on the basis of cell loss.

The increase in the relaxation time T2, which was seen in eight out of 11 patients (in one of them, possibly in relation to radiation therapy), has not been reported previously to our knowledge, and indicates an increased tissue water content (27). Nevertheless, the tumors were found to be contrast-enhancing. Therefore, it seems unlikely that the tumors were grossly cystic or necrotic. After 3–8 months of bromocriptine therapy, Gen et al (11) found atrophic tumor cells and signs of necrosis, with acellular spaces containing necrotic cells, hyaline substance, and fibrosis. These findings might explain our observation of an increasing T2, as the necrotic areas will probably have a large content of water. The persistent tumoral stroma with increasing perivascular fibrosis (12, 38) seems to explain the remaining contrast enhancement. In our opinion, therefore, both the marked tumor size reduction and the increase in T2 indirectly support the view that necrosis plays a part in the regression of some adenomas during long-term bromocriptine therapy.

After short-term treatment with bromocriptine (6 weeks), several investigators have found cell involution but no evidence of necrosis (7–10). We did not observe any significant alterations in relaxation times until after 1 year of therapy, and it is not clear whether the cell involution will result in any changes in the MR parameters. In two cases, however, a reduction of T2 was seen at an early stage, possibly reflecting dehydration due to reduction of the cell volume.

In addition to tumor reexpansion due to focal hemorrhage, reexpansion was seen in two patients, and, in one of them, there was radiologic and surgical evidence of regrowth of tumor tissue. Tumor regrowth during bromocriptine therapy has been reported previously, and has been attributed to resistance of cells to dopamine agonist action (40). In our case, T2 showed only a slight change, but this tumor could not be clearly distinguished from the others on the basis of the MR characteristics. In the other patient, there was a moderate diffuse increase in the signal intensity ratio in the T1-weighted image, together with a slight increase in T2. Positron emission tomography with ^{11}C-labeled methionine (41) indicated that the tumor was metabolically inactive, and, at transsphenoidal fine-needle aspiration, a small amount of hemorrhagic fluid was obtained. These findings might reflect diffuse hemorrhagic necrosis within the tumor (Muhr et al, unpublished data).

In our opinion, periodic MR imaging during bromocriptine therapy of macroprolactinomas is highly valuable to ensure that the treatment is effective, and for early detection of tumor reexpansion. Our study shows that reexpansion after an initial regression is not rare, and this may occur without an increase of S-PRL. Examination of the visual fields may be insensitive because of persisting defects after previous chiasmal compression. Invasive tumors may also expand laterally or inferiorly without compression of the visual pathways. The intervals between the MR examinations must be determined individually according to the therapeutic response. We suggest that, after the baseline examination, MR is performed at 1 month, 3 months, and 1 year, provided that there is tumor regression both clinically and radiologically. The intervals thereafter may often be longer and gradually increased, eg, 2–4 years, but with annual clinical check-ups. The MR studies should be performed with both frontal and sagittal images. The information that was unique to the T2-weighted images was valuable in cases with tumor reexpansion, but was otherwise primarily of scientific interest. Therefore, we propose that the baseline examination is carried out with both T1- and T2-weighted images, and that T1-weighted images may be sufficient during follow-up, unless tumor reexpansion or clinical deterioration occurs. Although based on a limited experience, we believe that enhancement with Gd-DTPA, in general, will not be necessary.

In conclusion, MR was highly useful for follow-up in bromocriptine therapy of macroprolactinomas, and provided new information regarding the optic chiasm, degenerative changes, and the water content in areas of apparently solid tumor tissue. New information on the long-term tumor size changes was also obtained.

References

1. Molitch ME, Elton RL, Blackwell RE, et al. Bromocriptine as primary therapy for prolactin-secreting macroadenomas: results of a prospective multicenter study. *J Clin Endocrinol Metab* 1985;60:698–705

2. Liuzzi A, Dallabonzana D, Oppizzi G, et al. Low doses of dopamine agonists in the long-term treatment of macroprolactinomas. *N Engl J Med* 1985;313:656–659
3. Chiodini P, Liuzzi A, Cozzi R, et al. Size reduction of macroprolactinomas by bromocriptine or lisuride treatment. *J Clin Endocrinol Metab* 1981;53:737–743
4. Scotti G, Scialfa G, Pieralli S, Chiodini PG, Spelta B, Dallabonzana D. Macroprolactinomas: CT evaluation of reduction of tumor size after medical treatment. *Neuroradiology* 1982;23:123–126
5. Wolpert SM. The radiology of pituitary adenomas. *Endocrinol Metab Clin* 1987;16:553–584
6. Hubbard JL, Scheithauer BW, Abboud CF, Laws ER Jr. Prolactin-secreting adenomas: the preoperative response to bromocriptine treatment and surgical outcome. *J Neurosurg* 1987;67:816–821
7. Rengachary SS, Tomita T, Jefferies BF, Watanabe I. Structural changes in human pituitary tumor after bromocriptine therapy. *Neurosurgery* 1982;10:242–251
8. Bassetti M, Spada A, Pezzo G, Giannattasio G. Bromocriptine treatment reduces the cell size in human macroprolactinomas: a morphometric study. *J Clin Endocrinol Metab* 1984;58:268–273
9. Tindall GT, Kovacs K, Horvath E, Thorner MO. Human prolactin-producing adenomas and bromocriptine: a histological, immunocytochemical, ultrastructural and morphometric study. *J Clin Endocrinol Metab* 1982;55:1178–1183
10. Barrow DL, Tindall GT, Kovacs K, Thorner MO, Horvath E, Hoffman JC Jr. Clinical and pathological effects of bromocriptine on prolactin-secreting and other pituitary tumors. *J Neurosurg* 1984;60:1–7
11. Gen M, Uozumi T, Ohta M, Ito A, Kajiwara H, Mori S. Necrotic changes in prolactinomas after long term administration of bromocriptine. *J Clin Endocrinol Metab* 1984;59:463–470
12. Mori H, Mori S, Saitoh Y, et al. Effects of bromocriptine on prolactin-secreting pituitary adenomas. *Cancer* 1985;56:230–238
13. Hallenga B, Saeger W, Lüdecke DK. Necroses of prolactin-secreting pituitary adenomas under treatment with dopamine agonists: light microscopical and morphometric studies. *Exp Clin Endocrinol* 1988; 92:59–68
14. Kaufman B, Kaufman BA, Arafah BM, Roessmann U, Selman WR. Large pituitary gland adenomas evaluated with magnetic resonance imaging. *Neurosurgery* 1987;21:540–546
15. Lundin P, Bergström K, Thuomas K-Å, Lundberg PO, Muhr C. Comparison of MR imaging and CT in pituitary macroadenomas. *Acta Radiol* 1991;32:189–196
16. Mikhael MA, Ciric IS. MR Imaging of pituitary tumors before and after surgical and/or medical treatment. *J Comput Assist Tomogr* 1988; 12:441–445
17. Pojunas KW, Daniels DL, Williams AL, Haughton VM. MR imaging of prolactin-secreting microadenomas. *AJNR* 1986;7:209–213
18. Weissbuch SS. Explanation and implications of MR signal changes within pituitary adenomas after bromocriptine therapy. *AJNR* 1986; 7:214–216
19. Yousem DM, Arrington JA, Zinreich SJ, Kumar AJ, Bryan RN. Pituitary adenomas: possible role of bromocriptine in intratumoral hemorrhage. *Radiology* 1989;170:239–243
20. Karnaze MG, Sartor K, Winthrop JD, Gabo MH, Hodges FJ III. Suprasellar lesions: evaluation with MR imaging. *Radiology* 1986; 161:77–82
21. Lundberg PO, Bergström K, Thuomas K-Å, Muhr C, Enoksson P. Magnetic resonance imaging of tumours of the sellar region: evaluation of treatment with bromocriptine retard. *Acta Radiol* 1986; (suppl 369):310–313
22. Lundberg PO, Drettner B, Hemmingsson A, Stenkvist B, Wide L. The invasive pituitary adenoma: a prolactin-producing tumor. *Arch Neurol* 1977;34:742–749
23. Scotti G, Yu C-Y, Dillon WP, et al. MR imaging of cavernous sinus involvement by pituitary adenomas. *AJR* 1988;151:799–806
24. Kaufman B, Tomsak RL, Kaufman BA, et al. Herniation of the suprasellar visual system and third ventricle into empty sellae: morphologic and clinical considerations. *AJR* 1989;152:597–608
25. Ostrov SG, Quencer RM, Hoffman JC, Davis PC, Hasso AN, David NJ. Hemorrhage within pituitary adenomas: how often associated with pituitary apoplexy syndrome? *AJNR* 1989;10:503–510
26. Dooms GC, Uske A, Brant-Zawadzki M, et al. Spin-echo MR Imaging of intracranial hemorrhage. *Neuroradiology* 1986;28:132–138
27. Kamman RL, Go KG, Brouwer W, Berendsen HJC. Nuclear magnetic resonance relaxation in experimental brain edema: effects of water concentration, protein concentration, and temperature. *Magn Reson Med* 1988;6:265–274
28. Sperber GO, Ericsson A, Hemmingsson A, Jung B, Thuomas K-Å. Improved formulae for signal amplitudes in repeated NMR sequences: application in NMR imaging. *Magn Reson Med* 1986;3:685–698
29. Clayton RN, Webb J, Heath DA, Dunn PJS, Rolfe EB, Hockley AD. Dramatic and rapid shrinkage of a massive invasive prolactinoma with bromocriptine: a case report. *Clin Endocrinol* 1985;22:573–581
30. Thorner MO, Martin WH, Rogol AD, et al. Rapid regression of pituitary prolactinoma during bromocriptine treatment. *J Clin Endocrinol Metab* 1980;51:438–445
31. Lundin P, Pedersen F. Volume of pituitary macroadenomas: assessment by MRI. *J Comput Assist Tomogr* (in press)
32. Weingarten K, Zimmerman RD, Deo-Narine V, Markisz J, Cahill PT, Deck MDF. MR imaging of acute intracranial hemorrhage: findings on sequential spin-echo and gradient-echo images in a dog model. *AJNR* 1991;12:457–467
33. Kjos BO, Brant-Zawadzki M, Kucharczyk W, Kelly WM, Norman D, Newton TH. Cystic intracranial lesions: magnetic resonance imaging. *Radiology* 1985;155:363–369
34. Glick RP, Tiesi JA. Subacute pituitary apoplexy: clinical and magnetic resonance imaging characteristics. *Neurosurgery* 1990;27:214–219
35. Onesti ST, Wisniewski T, Post KD. Clinical versus subclinical pituitary apoplexy: presentation, surgical management, and outcome in 21 patients. *Neurosurgery* 1990;26:980–986
36. Breger RK, Rimm AA, Fischer ME, Papke RA, Haughton VM. T1 and T2 measurements on a 1.5-T commercial MR imager. *Radiology* 1989;171:273–276
37. Kjos BO, Ehman RL, Brant-Zawadzki M, Kelly WM, Norman D, Newton TH. Reproducibility of relaxation times and spin density calculated from routine MR imaging sequences: clinical study of the CNS. *AJNR* 1985;6:271–276
38. Landolt AM, Osterwalder V. Perivascular fibrosis in prolactinomas: is it increased by bromocriptine? *J Clin Endocrinol Metab* 1984;58: 1179–1183
39. Esiri MM, Bevan JS, Burke CW, Adams CBT. Effect of bromocriptine treatment on the fibrous tissue content of prolactin-secreting and nonfunctioning macroadenomas of the pituitary gland. *J Clin Endocrinol Metab* 1986;63:383–388
40. Breidahl HD, Topliss DJ, Pike JW. Failure of bromocriptine to maintain reduction in size of a macroprolactinoma. *Br Med J* 1983;287: 451–452
41. Bergström M, Muhr C, Lundberg PO, Bergström K, Lundqvist H, Långström B. Amino acid metabolism in pituitary adenomas. *Acta Radiol* 1986;(suppl 369):412–414

Please see the Commentary by Kucharczyk on page 1293 in this issue.